Predictions for the properties of water below its homogeneous crystallization temperature revisited

Frédéric Caupin

14 (2022) 100090

Contents lists available at ScienceDirect

Journal of Non-Crystalline Solids: X

journal homepage: www.sciencedirect.com/journal/journal-of-non-crystalline-solids-x

Predictions for the properties of water below its homogeneous crystallization temperature revisited

Frédéric Caupin *

Institut Lumière Matière, Université de Lyon, Université Claude Bernard Lyon 1, CNRS, F-69622 Villeurbanne, France

ARTICLE INFO

Keywords:
Supercooled water
Kauzmann
Arrhenius
Adam-Gibbs
Angell

ABSTRACT

Properties of liquid water supercooled below its melting point have been thoroughly investigated. Experiments on bulk water become increasingly difficult as the temperature is lowered, and eventually impossible when the delay before ice nucleation becomes too short, around 230 K at ambient pressure. At low temperatures, amorphous ices and their glass transition may be studied only below the temperature of crystallization during heating, around 150 K. The temperature range from around 150 to 230 K at ambient pressure thus appears as a *no man's land* where the properties of bulk water are not accessible. Following Austen Angell's footsteps, I provide here physically acceptable predictions for thermodynamic properties (heat capacity, entropy) of liquid water down to its glass transition, and use the Adam-Gibbs approach to predict its dynamic properties (shear viscosity, self-diffusion coefficient, rotational correlation time).

1. Introduction

The last time I met Austen Angell was in Hamburg, during the DESY Water Week (25–28 February 2020), just before the outbreak of the covid-19 pandemic in Europe. Following my presentation, in which a slide showed a model predicting how much the heat capacity could increase in supercooled water [1], Austen was worried that most of the entropy of the supercooled liquid would be exhausted and would prematurely fall below that of ice, an accident known as the Kauzmann paradox [2]. In a later e-mail exchange, I sent him figures based on Ref. [1] showing that this was not the case; we shall see that my statement was too hasty. Austen suggested me to "to use [my] entropy variation with T to calculate the viscosity by the Adam-Gibbs equation, to see what it predicts."[1] Unfortunately, I could not find time to do so and show him the results. The purpose of this paper is to eventually present my "homework".

Viscosity was measured at ambient pressure down to 239 K [3]. The ice nucleation rate increases upon cooling, so that measurements at lower temperature become extremely difficult. The lowest temperature reached with bulk liquid water is around 230 K using fast evaporating droplets [4], and efforts with this technique have been recently made to obtain thermodynamic data [5,6]. To avoid crystallization of water and perform measurements at even lower temperature, tricks must be used, such as nanoscale confinement [7] or addition of solute [8] (see Ref. [9] for a review). However, the relation to the properties of pure bulk water is not straightforward [7,10]. On the low temperature side, measurements starting from the amorphous ices are limited by ice crystallization around 150 K at ambient pressure [11]. Therefore, a physically motivated prediction for the dynamic properties of water in the ≃150–230 K "no man's land" is valuable.

I will give here only a brief description of the salient points needed to understand the following, and refer the reader to classic references [12–14] for detailed reviews. The rapid decrease of entropy upon cooling is a common feature of many glassformers (the so-called fragile ones). Although it is not impossible for a liquid to reach a lower entropy than its crystalline counterpart (think about helium 3 at low temperature), this *entropy crisis* is puzzling enough to have led Kauzmann to suggest a possible thermodynamic origin for the glass transition [2]. The supercooled liquid would become a dynamically arrested phase (the glass) to stop loosing entropy. Entropy could thus control the dynamic properties of the supercooled liquid, and Adam and Gibbs [15] proposed a quantitative connection.

Such a connection between dynamics and thermodynamics has inspired many researchers, at the forefront of whom was Austen Angell. It is notable that his paper *On the Importance of the Metastable Liquid State and Glass Transition Phenomenon to Transport and Structure Studies in Ionic*

* Corresponding author.
E-mail address: frederic.caupin@univ-lyon1.fr.
[1] Austen Angell, in a personal email dated 23 March 2020

https://doi.org/10.1016/j.nocx.2022.100090
Received 30 November 2021; Received in revised form 15 February 2022; Accepted 9 March 2022
Available online 15 March 2022

Liquids. I. Transport Properties [16] was the eighth (out of 5105 at the time of writing) to cite Adam and Gibbs [15], within a year from its publication: the latter appeared on July 1, 1965, and the former was submitted to *The Journal of Physical Chemistry* on January 25, 1966. Since, Austen Angell constantly came back to the link between transport properties on the one hand, and heat capacity and entropy on the other hand, most recently in his work on phase change materials [17]. He first thought about applying the Adam-Gibbs approach to water in 1973 [18]. The large increase of heat capacity in supercooled water quickly reduces the liquid entropy. Constraining this entropy to remain higher than that of ice down to the glass transition temperature $T_g < 150\,K$ implies a λ-type anomaly for the heat capacity, which "would presumably be accompanied by a sharp drop in viscosity and diffusivity temperature dependences" [18]. This was reiterated by Angell et al. [19,20], who proposed that this would cause viscosity to change its fragile behavior near melting to a strong, Arrhenius behavior near T_g. Using constraints on the behavior of entropy and heat capacity near T_g and melting, Starr, Angell and Stanley [21] gave bounds for these quantities across the whole temperature range, and made predictions for the viscosity and self-diffusion coefficient. I will follow the same logic here, using a recent two-state model for the thermodynamics of stable and supercooled water [1].

The paper is organized as follows. Section 2 describes the sources used for the thermodynamic properties of water and ice, and compares their entropies, directly and in a Kauzmann plot. Section 3 presents experimental data for the dynamic properties of supercooled water, and displays their temperature dependence in an Arrhenius plot. Section 4 explores a possible connexion *à la* Adam-Gibbs between thermodynamic and dynamic quantities, and uses it to extrapolate dynamic data to low temperatures and plot them in an Angell plot. Section 5 discusses the results, with appropriate caveats.

2. Thermodynamic properties of supercooled water and ice: The Kauzmann plot

2.1. Thermodynamic properties of ice

Feistel and Wagner [22] have developed a Gibbs potential function for hexagonal ice, covering the ranges 0–273.16 K and 0–210 MPa. We use here only the thermodynamic values at ambient pressure ($P_{atm} = 101325\,Pa$) and down to 130 K, for which tables are provided. As the isobaric heat capacity $C_{P,\,ice}$ varies linearly in that range, we use the following function for the entropy of ice as a function of temperature:

$$S_{ice}(T) = S_{ref} + \int_{T_m}^{T} \frac{C_{P,ice}(T')}{T'}\,dT' = S_{ref} + a\left(\frac{T}{T_m} - 1\right) + bln\left(\frac{T}{T_m}\right), \tag{1}$$

where $T_m = 273.152519\,K$ is the melting point at P_{atm}, and $S_{ref} = -1220.76932549696\,J\,kg^{-1}\,K^{-1}$ the calculated entropy of ice at (T_m, P_{atm}). Fitting Eq. 1 on the 17 tabulated values from 130 to 273 K [22], we find: $a = 1912.21\,J\,kg^{-1}\,K^{-1}$ and $b = 173.407\,J\,kg^{-1}\,K^{-1}$.

2.2. Thermodynamic properties of supercooled water: A two-state approach

Liquid water is famous for its thermodynamic anomalies, such as its density maximum and isothermal compressibility and isobaric heat capacity maxima along isobars. The anomalous behavior becomes even more pronounced when the liquid is supercooled, that is at temperatures below ice-liquid equilibrium [23,24]. Two-state descriptions of water have a long history [25]. Water is viewed as a non-ideal mixture of two states A and B, in which the fraction x of the B state is not fixed, but a function of temperature and pressure which minimizes the total Gibbs free energy of the liquid. We have recently derived a two-state model [1] where the Gibbs free energy of the liquid reads:

$$G(T,P,x) = G_A + x[G_B(T,P) - G_A(T,P)] + k_B T[xlnx + (1-x)ln(1-x)] + \omega(P)x(1-x), \tag{2}$$

where G_A and G_B are the Gibbs free energies of liquids made of pure state A and pure state B, respectively; the third term is the ideal entropy of mixing, and the last term is the enthalpy of mixing for a regular solution. The model parameters were found by fitting above 1000 values of experimental data for liquid water in a broad range of temperatures and pressures: from 300 K to the temperature of homogeneous ice nucleation, and from 400 MPa to the pressure of homogeneous vapor nucleation. The resulting fit describes all data within their uncertainties. We tested two versions of this model, with and without including recent, indirect isothermal compressibility data from experiments on fast evaporating micrometer-sized droplets [5]. We have argued [26] that these data might suffer some bias in the compressibility or temperature [4] values. Indeed, the slope of the compressibility-temperature curve from Ref. [5] does not match that from a previous work by Kanno and Angell using capillaries 200μm in diameter [27] in the temperature range where the two sets overlaps (see Fig. 7 of Ref. [1]). As including the data from Ref. [5] causes systematic deviations in the fit, in the following, we will use the version without them.

Introducing the "reaction constant" K such that $k_B T \ln K = G_B - G_A$, the equilibrium fraction x_e is found by minimizing G:

$$k_B T\left(lnK + ln\frac{x_e}{1-x_e}\right) + \omega(P)(1-2x_e) = 0. \tag{3}$$

As shown in Ref. [1], x_e switches from 0 to 1 when the temperature is lowered, so that the system changes from an A-like liquid at high-temperature to a B-like liquid at low temperature. At high pressure, the change in x_e is discontinuous, signaling a first-order liquid-liquid transition ending at a critical point around 218 K and 72 MPa. Note that this is a prediction from the model, as all supporting experimental data were measured at state points above the putative transition. At lower pressures, x_e changes continuously, with an inflection point at $x_e = 1/2$ which defines the so-called Widom line associated with the liquid-liquid transition [24].

From Eq. 2, the entropy S and isobaric heat capacity C_P follow:

$$S = -\left(\frac{\partial G}{\partial T}\right)_P = S_A - k_B\left[x_e\left(\frac{\partial(TlnK)}{\partial T}\right)_P + x_e lnx_e + (1-x_e)ln(1-x_e)\right], \tag{4}$$

$$C_P = T\left(\frac{\partial S}{\partial T}\right)_P = C_{P,A} - k_B T\left\{x_e\left(\frac{\partial^2(TlnK)}{\partial T^2}\right)_P + \left(\frac{\partial x_e}{\partial T}\right)_P\left[\left(\frac{\partial(TlnK)}{\partial T}\right)_P + ln\frac{x_e}{1-x_e}\right]\right\}, \tag{5}$$

where S_A and $C_{P,\,A}$ are the entropy and isobaric heat capacity of a pure state A liquid, respectively. When preparing the present article, I discovered a discrepancy between the entropy variation calculated by integration of C_P/T and by direct difference. I found out that it arose from an error in the version of Eq. 4 used in Ref. [1]. Fortunately, S was not directly used in the fit of experimental data, and the expressions for all other quantities were correct; therefore the results of Ref. [1] are unaffected, except for the entropy displayed in its Figs. 17 and S6[2]; corrected versions of these figures have now appeared in an Erratum [28]. The correct expression for S, Eq. 4, is used here.

At ambient pressure, the fitted data extend down to 239.75 K. Fig. 1 compares this model and its extrapolation to lower temperatures to ice and to the previous work by Starr et al. [21]. We see that the various models for the liquid all exhibit a heat capacity maximum of similar

[2] These are the figures I sent to Austen Angell.

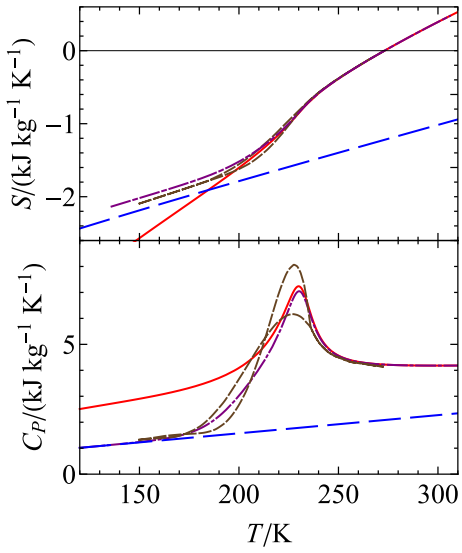

Fig. 1. Top: entropy as a function of temperature for ice (long-dashed blue) and liquid water (solid red: Ref. [1], short-dashed brown: bounds from Ref. [21]). The ice curve is the fit with Eq. 1 to data from an empirical equation of state for hexagonal ice [22]. The liquid curve is based on a two-state fit to experimental data [1], down to 240 K for entropy, and extrapolated below. The curves intersect at 184.49 K. To avoid this crossing, and keep the liquid entropy above that of the crystal, a switching function (Eq. 6) is introduced; the modified liquid entropy is shown as a dot-dashed purple curve. Bottom: isobaric heat capacity as a function of temperature; the legend is the same as in the top panel. (For interpretation of the references to colour in this figure legend, the reader is referred to the web version of this article.)

magnitude, which translates into an inflection point in the entropy curve. In the two-state model, the maximum and inflection point occur near the Widom line. The good agreement between two independent methods (the two-state prediction based only on high temperature data, and the estimate from Ref. [21], based on polynomial interpolation between constrained behaviors at high and low temperature) is remarkable. A departure is seen only at the lowest temperatures, when the prediction for C_P from Ref. [21] reaches the ice value, while that from the two-state extrapolation remains at higher values. Accordingly, the entropy from the two-state extrapolation keeps dropping to lower values than that from Ref. [21], and the former crosses the entropy of ice at 184.49 K. In the two-state model, C_P of the liquid asymptotically approaches C_P of state B at low temperature. If one wishes to avoid the early crossing of the entropies of supercooled water and ice, C_P for state B in the two-state model should be constrained to lie above C_P of ice. This should be possible with an appropriate modification of $G_B - G_A$ in Eq. 2. I leave this for future work, and for the time being I simply introduce a switching function ϕ to modify the C_P behavior at low temperature, viz. $C_P^*(T) = \phi(T)C_P(T) + [1 - \phi(T)]C_{P,\,\mathrm{ice}}(T)$, with

$$\phi(T) = \frac{1}{2}\left[1 + tanh\frac{T - T_{\mathrm{switch}}}{\delta T}\right]. \tag{6}$$

The modified entropy S^* follows by integrating C_P^*/T. Fig. 1 shows with a dot-dashed purple curve S^* and C_P^* using $T_{\mathrm{switch}} = 197$ K and $\delta T = 20$ K. At 244.11 K, the lowest temperature for which accurate C_P data is available, C_P^* is lower than C_P by 0.55% only, so that the quality of the two-state model in representing experimental data remains unaffected. C_P^* is now close to the lower estimate from Ref. [21], and, by design, S^* now remains above S_{ice}, with a difference approximately twice that proposed in Ref. [21]. The latter used the mean value for S_{ex} reported by Speedy et al. in Ref. [29]. From the study of evaporation rates of amorphous water and ice, they estimated $S_{\mathrm{ex}} = 94 \pm 94\,\mathrm{J\,kg^{-1}K^{-1}}$ at 150 K; the value for $S^* - S_{\mathrm{ice}}(150\,\mathrm{K}) = 168\,\mathrm{J\,kg^{-1}K^{-1}}$ is not incompatible. We shall see that it leads to predictions significantly different from Ref. [21].

2.3. The Kauzmann plot

With the entropies for ice (Section 2.1) and liquid (Section 2.2), we can now define the excess entropy S_{ex}=S-S_{ice} and build the Kauzmann plot, displaying $S_{\mathrm{ex}}(T)/S_{\mathrm{ex}}(T_{\mathrm{m}})$ as a function of T/T_{m} (Fig. 2, top). Down to 0.8 T_{m}, all choices for the liquid entropy stay very close; at lower temperatures, the raw S from the two-state model gives an unphysical $S_{\mathrm{ex}} = 0$ above T_{g}, whereas the corrected S^* and S from Ref. [21] turn around, avoiding the entropy crisis.

Angell introduced an alternate version of the Kauzmann plot, the "thermodynamic fragility" plot. The quantities are now scaled with respect to T_{g} rather than to T_{m}, and the slope corresponds to the fragility. The result is displayed in Fig. 2 (bottom), except for the raw two-state prediction for S, which crosses S_{ice} above T_{g} and cannot be shown with this representation. We have used throughout the present work $T_{\mathrm{g}} = 136$ K. Within the extrapolations used, water changes from a very fragile behavior near T_{m} to a strong behavior near T_{g}. When compared to other glassformers (see Fig. 2 of Ref. [21]), water would be the strongest liquid near T_{g}.

3. Dynamic properties of supercooled water: The Arrhenius plot

Shear viscosity η, self-diffusion coefficient D, and rotational correlation time τ_{r} have been extensively measured in supercooled water. In their seminal 1976 paper [30], Speedy and Angell showed that, at ambient pressure, these dynamic quantities, as well as thermodynamic

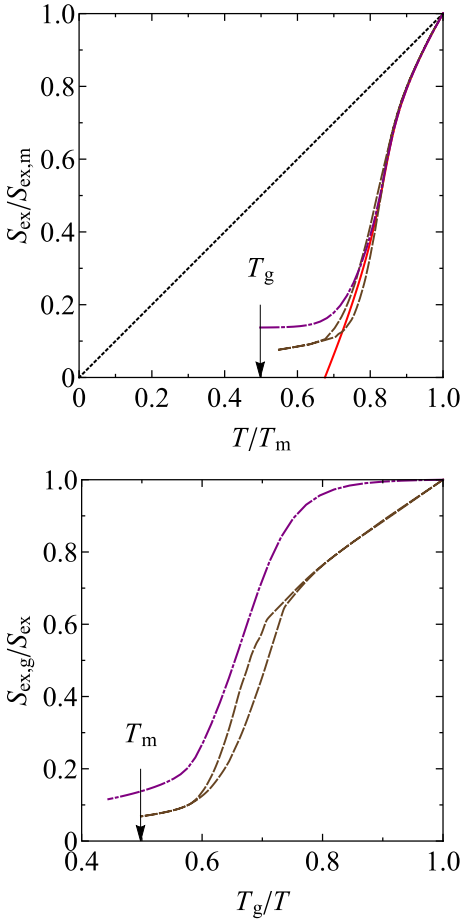

Fig. 2. Kauzmann (top) and thermodynamic fragility (bottom) plots. The legend is the same as in Fig. 1. The dotted line in the top panel shows the first bisector.

quantities, can be described by the power-law

$$A(T) = A_0 \left(\frac{T}{T_s} - 1 \right)^{-\gamma}. \quad (7)$$

Later measurements of D in supercooled water at ambient pressure [31,32] were found to be better described by such a power-law than by the Vogel-Tamman-Fulcher (VTF) relationship $A(T) = A_0 \exp[-B/(T - T_0)]$ traditionally used to describe fragile glassformers. Recently, we obtained viscosity data of deeply supercooled water from the Brownian motion of colloids [3]. Using a compilation of literature shear viscosity (including our new data), self-diffusion coefficient, and rotational correlation time, we confirmed that the power-law (Eq. 7) performs better than VTF, and gives a representation of experimental data within their uncertainty over a broad temperature range. For easy reference, the best-fit parameters and fitted region given in Ref. [3] are reproduced here in Table 1. Using these fits, we plot in an Arrhenius plot (Fig. 3) the three dynamic quantities from 300 K to the lowest measured temperatures (red curves). Simulations of η and D for the TIP4P/2005 water model [33,34] are in good agreement with experimental data, and extend to lower temperatures (see Section 4). The behavior is super-Arrhenius, making water at moderate supercooling a fragile liquid.

We note that mode-coupling theory (MCT) [35] predicts for dynamic quantities in moderately supercooled liquids a power-law behavior as in Eq. 7. MCT predictions have been confirmed in simulation studies of water (see e.g. Refs. [36–38]). However, as discussed in Ref. [3], the differences in the singular temperature T_s and in the absolute values of the power-law exponent γ (Table 1) are not in line with all MCT predictions.

4. A link between dynamics and thermodynamics?

A long-standing idea in the field of the glass transition is a possible link between thermodynamics, in particular the Kauzmann paradox, and dynamics. The dynamic arrest of the glassformer would be due to the approach of the entropy crisis at T_K, with dynamic processes involving increasingly larger cooperatively rearranging regions as T_K is approached. This is formalized in the Adam-Gibbs theory by writing:

$$A(T) = A_0 exp\left(\frac{B}{TS_{conf}(T)} \right), \quad (8)$$

where A is a dynamic quantity, A_0 a prefactor, B an energy parameter, and S_{conf} measures the configurational entropy (that is liquid entropy left when vibrational contributions have been subtracted).

4.1. Configurational entropy

To test Eq. 8, the first step is to define a proxy for S_{conf}. It is common to assume that vibrational contributions are identical in the liquid and the crystal (see however Section 5), and to write S_{conf} as the excess entropy S_{ex} (the difference between the entropies in the two phases):

$$S_{conf} = S_{ex} = S - S_{ice}. \quad (9)$$

In the case of ice, Starr et al. [21] argued that the above equation unnecessarily removes the residual entropy due to proton disorder in ice $S_{res} = k_B \ln(3/2)$, and thus wrote:

Table 1
Best fits obtained with a power-law $A_0(T/T_s - 1)^{-\gamma}$ [3].

Quantity	Temperature range (K)	T_s (K)	γ	A_0
Viscosity η	239.15–373.15	225.66	1.6438	137.88 μPas
Self-diffusion coefficient D	237.8–498.2	213.96	−2.0801	16077 $\mu m^2 s^{-1}$
Rotational relaxation time τ_r	236.18–451.63	223.05	1.8760	217.89 fs

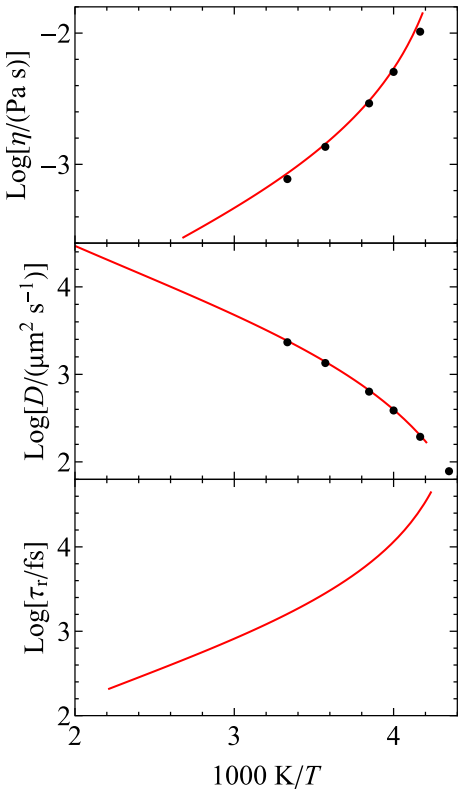

Fig. 3. Arrhenius plots showing the base-10 logarithm of a dynamic quantity (viscosity η: top; self-diffusion coefficient D: middle; rotational correlation time τ_r: bottom) as a function of inverse temperature. The red curves are accurate power-law fits to experimental data (with parameters given in Table 1), plotted to the lowest temperature at which experiments were performed. The black discs display the results of simulations of η and D with the TIP4P/2005 water model [34]. (For interpretation of the references to colour in this figure legend, the reader is referred to the web version of this article.)

$$S_{conf} = S_{ex} + S_{res}. \quad (10)$$

4.2. Correlation with dynamic properties: The Adam-Gibbs plot

To assess the performance of the Adam-Gibbs equation (Eq. 8), we plot the base-10 logarithm of dynamic properties (Section 3) as a function of $1/(TS_{conf})$. Fig. 4 displays the results when respectively not including (Eq. 9, left panels) or including (Eq. 10, right panels) S_{res} in S_{conf}. Note that we have used data from 300 K to the lowest experimental temperature for a dynamic quantity. To calculate S_{conf}, we have therefore used the two-state model for S and Eq. 1 for S_{ice} (which involves a short extrapolation above the melting point). We have then performed a linear fit to the data, sampling evenly 20 points along the horizontal axis. In all cases, the behavior is remarkably linear, with a better linearity in the case where S_{res} is included in S_{conf}. We will thus follow Starr et al. and use Eq. 10 for S_{conf} in the following. The parameters for the linear fit to the various dynamic properties are given in Table 2.

4.3. Prediction for dynamics at low temperature

We have now all the ingredients to give predictions for the dynamic properties of water at low temperature. To extrapolate the liquid entropy, we use the various choices presented in Section 2.2. We then calculate each dynamic quantity from the extrapolation of the linear fits displayed in Fig. 4 (right panels) (with parameters given in Table 2). The results are displayed in Fig. 5 in the form of an Angell plot showing the base-10 logarithm of dynamic properties as a function of T_g/T.

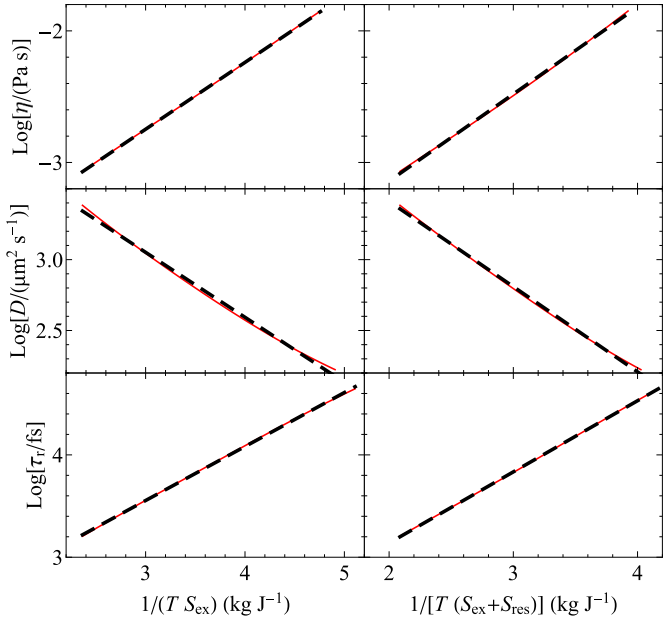

Fig. 4. Adam-Gibbs plot for a dynamic quantity (viscosity η: top; self-diffusion coefficient D: middle; rotational correlation time τ_r: bottom) as a function of $1/(TS_{conf})$, using Eq. 9 (left column) or Eq. 10 (right column) for S_{conf}. The solid red curve and dashed black line show the experimental data and a linear fit, respectively. (For interpretation of the references to colour in this figure legend, the reader is referred to the web version of this article.)

Table 2
Best linear fits to the base-10 logarithm of each dynamic quantity in the indicated units with $\alpha + \beta/(TS_{conf})$, with S_{conf} from Eq. 10.

Dynamic quantity	Units	α	$\beta/(\mathrm{J kg^{-1}})$
Viscosity η	Pa s	−4.271	0.5080
Self-diffusion coefficient D	$\mu m^2 s^{-1}$	4.427	−0.4584
Rotational correlation time τ_r	fs	1.972	0.5275

While the experimental data for the stable and supercooled liquid are well described by a Speedy-Angell power-law, its extrapolation suggests a surprising divergence at T_s near 220 K, which seems unphysical if liquid water is connected to the low-density amorphous ice at T_g = 136 K. Using the Adam-Gibbs approach with the various models for S_{conf} based on the shape of the heat capacity of supercooled water allows avoiding the divergence. This was the idea introduced in the seminal works by Angell et al. [18,20,21]. However, as they constrained S_{ex} to reach a rather low value close to 150 K, they obtained predictions for η and D reaching extreme values far above T_g (brown long-dashed curves in Fig. 5). The behavior is even more extreme when the raw prediction from the two-state model [1] is used (solid red curve), as S_{ex} vanishes at 184.49 K (see Section 2.2). Correcting the prediction for S from the two-state model into S^* using the switching function (Eq. 6) removes the singularity (dot-dashed purple curve). In fact, I have manually chosen the values for T_{switch} and δT to match the self-diffusion coefficient experimentally obtained from analysis of the growth rate of ice in thin water films (a few tens of monolayers) [39] (long-dashed black curve in Fig. 5 middle panel); interestingly, these experimental data for D agree with simulations. A good match is obtained with a physically acceptable shape for S^* and C_P^* (Fig. 1). We note that Shi et al. [41] also obtained a good representation of the D data on thin water films [39], using another two-state model where the enthalpy of mixing in Eq. 2 is neglected. In their model, there is thus no liquid-liquid transition nor Widom line. Another difference is that they do not use the Adam-Gibbs approach to obtain dynamic quantities, but rather an Arrhenius law in which the activation energy depends linearly on the fraction of the two states.

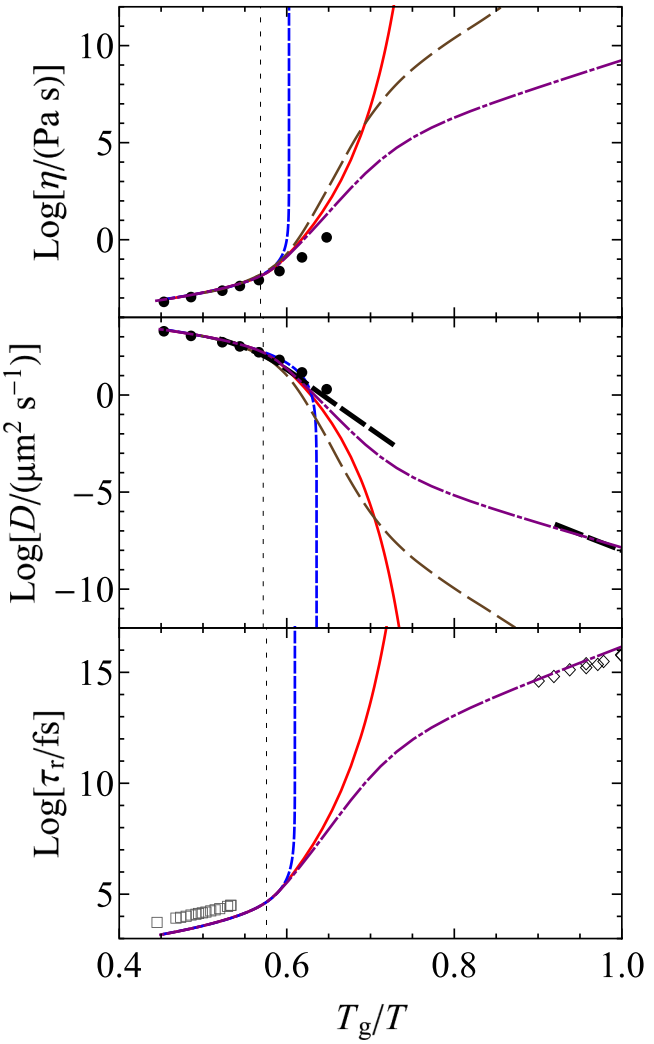

Fig. 5. Angell plot showing the base-10 logarithm of a dynamic quantity (viscosity η: top; self-diffusion coefficient D: middle; rotational correlation time τ_r: bottom) as a function of T_g/T. The lowest temperature at which experimental data are available is indicated by a vertical dotted line. Several extrapolations are shown: Speedy-Angell power-law (Eq. 7, short-dashed blue), and Adam-Gibbs equation (Eq. 8) using the liquid entropy from Ref. [21] (long-dashed brown), from the two-state model [1] (solid red) and its modified version (S^*, Section 2.2, dot-dashed purple). The black discs in the top and middle panels show results of simulations with the TIP4P/2005 water model [34]. The long-dashed, thick black curve in the middle panel shows D estimated from the growth rate of ice in thin water films (a few tens of monolayers) [39]. The gray empty squares and black empty diamonds in the bottom panel shows dielectric relaxation time from Refs. [11,40], respectively. (For interpretation of the references to colour in this figure legend, the reader is referred to the web version of this article.)

There is no exprimental η or τ_r data available close to T_g. However, dielectric relaxation times τ_D have been measured when heating low-density amorphous ice [11]. As dielectric relaxation time measured for stable and supercooled water [40] are roughly proportional to τ_r (the ratio varies between 4.66 and 5.05 in the range 255 K to 305.5 K), dielectric data may be used as a rough proxy for τ_r. The τ_r prediction from S^* turns out to be very close to the measured dielectric data at low temperature. The behavior predicted with S^* for all three properties is a transition from a fragile liquid close to T_m to a very strong one close to T_g, as hypothesized by Angell et al. [19,20]. The fragility index, defined as the slope in the Angell plot near T_g is 13.9, 12.7, and 14.7 for η, D, and

τ_r, respectively, in good agreement with the value 14 reported for dielectric data [11].

5. Discussion

Dynamic properties of water exhibit a fragile, super-Arrhenius variation upon cooling (Fig. 3), well described by a power-law, which suggests a divergence at T_s near 220 K. Simulation data [33,34] suggest that there is no such divergence. Data on the self-diffusion coefficients [39] and dielectric relaxation time [11] near T_g also suggest an Arrhenius behavior at low temperature with a low activation energy, making water one of the strongest liquids. To avoid the divergence and turn from fragile to strong, the dynamic behavior of water should thus change drastically around 220 K. Unfortunately, this temperature region lies in the *no man's land* [9,42]: experiments cannot be performed below the temperature of homogeneous ice nucleation (around 230 K [4]), nor above the temperature of crystallization upon heating of the amorphous phases of water (around 150 K [11]).

This has prompted Austen Angell and others to look for predictions of dynamic properties in the *no man's land* based on the Adam-Gibbs approach. The Adam-Gibbs dependence of the dynamic properties on the configuration entropy is well obeyed in water down to the homogeneous ice nucleation temperature (Fig. 4). It is a matter of assumption to use its extrapolation for covering over 10 orders of magnitude of further changes. Simulations have been performed to test this assumption with water models. For instance, in Ref. [43], the logarithm of the self-diffusion coefficient was found to follow $1/(TS_{conf})$ over 3 orders of magnitude. However, further tests have been recently performed over a much broader range with simulated models (hard spheres, soft spheres, and soft disks) [44]. The conclusion was that the Adam-Gibbs relation is generally violated. We note however that the dynamic property investigated was the relaxation time τ_α rather than η, D, or τ_r. We note also that, except for hard spheres, the deviation from linearity of $\log\tau_\alpha$ vs. $1/(TS_{conf})$ remains moderate, around 2 orders of magnitude for a total variation spanning 9 orders of magnitude.

A serious issue with the experimental approach is the identification of S_{conf} with S_{ex} (Eq. 9) or $S_{ex} + S_{res}$ (Eq. 10). It has often been stated that this is based on the assumption that the vibrational contribution to the entropy is the same in the liquid and crystal phases, which is unfortunately not the case [45]. Angell and Borick [46] gave experimental, simulations, and analytic arguments supporting that, although different, excess entropy and configurational entropy would remain proportional, which would thus preserve the Adam-Gibbs relation. After recalling this argument in Ref. [13], Angell wrote: "Regardless of the truth of the latter statement, it is reasonable to test relationships using the 'modified' Adam-Gibbs equation in which, faute-de-mieux, the excess entropy is employed." Indeed, experiments don't have access to all the tools available in simulations, where S_{conf} can be obtained e.g. from the potential energy landscape [43,47] or the entropy difference between liquid and glass [44]. It might well be that the proportionality between S_{ex} and S_{conf} starts to fail at low temperature, as suggested by the analysis of simulations with the TIP4P/2005 water model [48].

Keeping in mind the above caveats about the applicability of the Adam-Gibbs relation and the definition of the configurational entropy, it remains fascinating to see how a simple expression connecting thermodynamic and dynamic quantities may yield predictions connecting the behavior of liquid water at small and large supercooling, all the way through the *no man's land*. I leave the conclusion to Austen; in his early paper [16], where he called T_0 the temperature at which S_{conf} vanishes, he wrote: "If the essential characteristic of the liquid state, viz. its configurational entropy, does not vanish before T_0, then the temperature range from the melting point down to T_0 is as equally valid a part of the liquid state as the range melting point to boiling point: to date, then, investigators of the post-melting point range have not had the benefit of any understanding of the behavior of this lower part of the ionic liquid range on which to build."

Declaration of Competing Interest

The authors declare that they have no known competing financial interests or personal relationships that could have appeared to influence the work reported in this paper.

Acknowledgments

Support from Agence Nationale de la Recherche, grant number ANR-19-CE30-0035-1, is acknowledged. I dedicate this work to the memory of C. Austen Angell, whose achievements, constant enthusiasm and encouragements have been to me a tremendous source of inspiration.

References

[1] F. Caupin, M.A. Anisimov, Thermodynamics of supercooled and stretched water: unifying two-structure description and liquid-vapor spinodal, J. Chem. Phys. 151 (3) (2019), https://doi.org/10.1063/1.5100228, 034503.
[2] W. Kauzmann, The nature of the glassy state and the behavior of liquids at low temperatures, Chem. Rev. 43 (2) (1948) 219–256, https://doi.org/10.1021/cr60135a002.
[3] A. Dehaoui, B. Issenmann, F. Caupin, Viscosity of deeply supercooled water and its coupling to molecular diffusion, Proc. Natl. Acad. Sci. 112 (39) (2015) 12020–12025, https://doi.org/10.1073/pnas.1508996112.
[4] C. Goy, M.A.C. Potenza, S. Dedera, M. Tomut, E. Guillerm, A. Kalinin, K.-O. Voss, A. Schottelius, N. Petridis, A. Prosvetov, G. Tejeda, J.M. Fernández, C. Trautmann, F. Caupin, U. Glasmacher, R.E. Grisenti, Shrinking of rapidly evaporating water microdroplets reveals their extreme supercooling, Phys. Rev. Lett. 120 (1) (2018), https://doi.org/10.1103/PhysRevLett.120.015501, 015501.
[5] K.H. Kim, A. Späh, H. Pathak, F. Perakis, D. Mariedahl, K. Amann-Winkel, J. A. Sellberg, J.H. Lee, S. Kim, J. Park, K.H. Nam, T. Katayama, A. Nilsson, Maxima in the thermodynamic response and correlation functions of deeply supercooled water, Science 358 (6370) (2017) 1589–1593, https://doi.org/10.1126/science.aap8269.
[6] H. Pathak, A. Späh, N. Esmaeildoost, J.A. Sellberg, K.H. Kim, F. Perakis, K. Amann-Winkel, M. Ladd-Parada, J. Koliyadu, T.J. Lane, C. Yang, H.T. Lemke, A. R. Oggenfuss, P.J.M. Johnson, Y. Deng, S. Zerdane, R. Mankowsky, P. Beaud, A. Nilsson, Enhancement and maximum in the isobaric specific-heat capacity measurements of deeply supercooled water using ultrafast calorimetry, Proc. Natl. Acad. Sci. U. S. A. 118 (6) (2021), https://doi.org/10.1073/pnas.2018379118 e2018379118.
[7] S. Cerveny, F. Mallamace, J. Swenson, M. Vogel, L. Xu, Confined water as model of supercooled water, Chem. Rev. 116 (13) (2016) 7608–7625, https://doi.org/10.1021/acs.chemrev.5b00609.
[8] S. Woutersen, B. Ensing, M. Hilbers, Z. Zhao, C.A. Angell, A liquid-liquid transition in supercooled aqueous solution related to the HDA-LDA transition, Science 359 (6380) (2018) 1127–1131, https://doi.org/10.1126/science.aao7049.
[9] F. Caupin, Escaping the no man's land: recent experiments on metastable liquid water, J. Non-Cryst. Solids 407 (2015) 441–448, https://doi.org/10.1016/j.jnoncrysol.2014.09.037.
[10] J. Bachler, L.-R. Fidler, T. Loerting, Absence of the liquid-liquid phase transition in aqueous ionic liquids, Phys. Rev. E 102 (6) (2020), https://doi.org/10.1103/PhysRevE.102.060601, 060601.
[11] K. Amann-Winkel, C. Gainaru, P.H. Handle, M. Seidl, H. Nelson, R. Bohmer, T. Loerting, Water's second glass transition, Proc. Natl. Acad. Sci. U. S. A. 110 (44) (2013) 17720–17725, https://doi.org/10.1073/pnas.1311718110.
[12] C.A. Angell, Formation of glasses from liquids and biopolymers, Science 267 (5206) (1995) 1924–1935, https://doi.org/10.1126/science.267.5206.1924.
[13] C.A. Angell, Liquid fragility and the glass transition in water and aqueous solutions, Chem. Rev. 102 (8) (2002) 2627–2650, https://doi.org/10.1021/cr000689q.
[14] M.D. Ediger, Perspective: highly stable vapor-deposited glasses, J. Chem. Phys. 147 (21) (2017) 210901, https://doi.org/10.1063/1.5006265.
[15] G. Adam, J.H. Gibbs, On the temperature dependence of cooperative relaxation properties in glass-forming liquids, J. Chem. Phys. 43 (1) (1965) 139–146. http://scitation.aip.org/content/aip/journal/jcp/43/1/10.1063/1.1696442.
[16] C.A. Angell, On the importance of the metastable liquid state and glass transition phenomenon to transport and structure studies in ionic liquids. I. Transport properties 1, J. Phys. Chem. 70 (9) (1966) 2793–2803, https://doi.org/10.1021/j100881a014.
[17] S. Wei, P. Lucas, C.A. Angell, Phase change alloy viscosities down to T_g using Adam-Gibbs-equation fittings to excess entropy data: a fragile-to-strong transition, J. Appl. Phys. 118 (3) (2015), https://doi.org/10.1063/1.4926791, 034903.
[18] C.A. Angell, J. Shuppert, J.C. Tucker, Anomalous properties of supercooled water. Heat capacity, expansivity, and proton magnetic resonance chemical shift from 0 to −38%, J. Phys. Chem. 77 (26) (1973) 3092–3099, https://doi.org/10.1021/j100644a014.
[19] C.A. Angell, Water II is a "strong" liquid, J. Phys. Chem. 97 (24) (1993) 6339–6341, https://doi.org/10.1021/j100126a005.
[20] K. Ito, C.T. Moynihan, C.A. Angell, Thermodynamic determination of fragility in liquids and a fragile-to-strong liquid transition in water, Nature 398 (6727) (1999) 492–495, https://doi.org/10.1038/19042.

[21] F.W. Starr, C. Angell, H. Stanley, Prediction of entropy and dynamic properties of water below the homogeneous nucleation temperature, Phys. A Stat. Mech. Appl. 323 (2003) 51–66, https://doi.org/10.1016/S0378-4371(03)00012-8.
[22] R. Feistel, W. Wagner, A new equation of state for H2O ice Ih, J. Phys. Chem. Ref. Data 35 (2) (2006) 1021–1047, https://doi.org/10.1063/1.2183324.
[23] P.G. Debenedetti, Supercooled and glassy water, J. Phys. Condens. Matter 15 (45) (2003) R1669–R1726, https://doi.org/10.1088/0953-8984/15/45/R01.
[24] P. Gallo, K. Amann-Winkel, C.A. Angell, M.A. Anisimov, F. Caupin, C. Chakravarty, E. Lascaris, T. Loerting, A.Z. Panagiotopoulos, J. Russo, J.A. Sellberg, H.E. Stanley, H. Tanaka, C. Vega, L. Xu, L.G.M. Pettersson, Water: a tale of two liquids, Chem. Rev. 116 (13) (2016) 7463–7500, https://doi.org/10.1021/acs.chemrev.5b00750.
[25] M.A. Anisimov, M. Duška, F. Caupin, L.E. Amrhein, A. Rosenbaum, R.J. Sadus, Thermodynamics of fluid polyamorphism, Phys. Rev. X 8 (1) (2018), https://doi.org/10.1103/PhysRevX.8.011004, 011004.
[26] F. Caupin, V. Holten, C. Qiu, E. Guillerm, M. Wilke, M. Frenz, J. Teixeira, A. K. Soper, Comment on "maxima in the thermodynamic response and correlation functions of deeply supercooled water", Science 360 (6390) (2018) https://doi.org/10.1126/science.aat1634 eaat1634.
[27] H. Kanno, C.A. Angell, Water: Anomalous compressibilities to 1.9 kbar and correlation with supercooling limits, J. Chem. Phys. 70 (9) (1979) 4008–4016, https://doi.org/10.1063/1.438021.
[28] F. Caupin, M.A. Anisimov, Erratum: "Thermodynamics of supercooled and stretched water: unifying two-structure description and liquid-vapor spinodal", J. Chem. Phys. 151 (2019) https://doi.org/10.1063/5.0085566, 034503. J. Chem. Phys. 156 (6) (2022) 069902.
[29] R.J. Speedy, P.G. Debenedetti, R.S. Smith, C. Huang, B.D. Kay, The evaporation rate, free energy, and entropy of amorphous water at 150 K, J. Chem. Phys. 105 (1) (1996) 240–244, https://doi.org/10.1063/1.471869.
[30] R.J. Speedy, C.A. Angell, Isothermal compressibility of supercooled water and evidence for a thermodynamic singularity at −45°C, J. Chem. Phys. 65 (3) (1976) 851–858, https://doi.org/10.1063/1.433153.
[31] F.X. Prielmeier, E.W. Lang, R.J. Speedy, H.-D. Lüdemann, Diffusion in supercooled water to 300 MPa, Phys. Rev. Lett. 59 (10) (1987) 1128–1131, https://doi.org/10.1103/PhysRevLett.59.1128.
[32] W.S. Price, H. Ide, Y. Arata, Self-diffusion of supercooled water to 238K using PGSE NMR diffusion measurements, J. Phys. Chem. A 103 (4) (1999) 448–450, https://doi.org/10.1021/jp9839044.
[33] P. Montero de Hijes, E. Sanz, L. Joly, C. Valeriani, F. Caupin, Viscosity and self-diffusion of supercooled and stretched water from molecular dynamics simulations, J. Chem. Phys. 149 (9) (2018), https://doi.org/10.1063/1.5042209, 094503.
[34] S. Dueby, V. Dubey, S. Daschakraborty, Decoupling of translational diffusion from the viscosity of supercooled water: role of translational jump diffusion, J. Phys. Chem. B 123 (33) (2019) 7178–7189, https://doi.org/10.1021/acs.jpcb.9b01719.
[35] W. Gotze, L. Sjogren, Relaxation processes in supercooled liquids, Rep. Prog. Phys. 55 (3) (1992) 241–376. http://iopscience.iop.org/0034-4885/55/3/001.
[36] P. Gallo, F. Sciortino, P. Tartaglia, S.-H. Chen, Slow dynamics of water molecules in supercooled states, Phys. Rev. Lett. 76 (15) (1996) 2730–2733. http://journals.aps.org/prl/abstract/10.1103/PhysRevLett.76.2730.
[37] F.W. Starr, F. Sciortino, H.E. Stanley, Dynamics of simulated water under pressure, Phys. Rev. E 60 (6) (1999) 6757–6768, https://doi.org/10.1103/PhysRevE.60.6757.
[38] M. De Marzio, G. Camisasca, M. Rovere, P. Gallo, Mode coupling theory and fragile to strong transition in supercooled TIP4P/2005 water, J. Chem. Phys. 144 (7) (2016), https://doi.org/10.1063/1.4941946, 074503.
[39] Y. Xu, N.G. Petrik, R.S. Smith, B.D. Kay, G.A. Kimmel, Growth rate of crystalline ice and the diffusivity of supercooled water from 126 to 262 K, Proc. Natl. Acad. Sci. U. S. A. 113 (52) (2016) 14921–14925, https://doi.org/10.1073/pnas.1611395114.
[40] D. Bertolini, M. Cassettari, G. Salvetti, The dielectric relaxation time of supercooled water, J. Chem. Phys. 76 (6) (1982) 3285–3290, https://doi.org/10.1063/1.443323.
[41] R. Shi, J. Russo, H. Tanaka, Origin of the emergent fragile-to-strong transition in supercooled water, Proc. Natl. Acad. Sci. 115 (38) (2018) 9444–9449, https://doi.org/10.1073/pnas.1807821115.
[42] O. Mishima, H.E. Stanley, The relationship between liquid, supercooled and glassy water, Nature 396 (6709) (1998) 329–335. http://www.nims.jp/water/Publications/MS1998nature-b.pdf.
[43] P.H. Handle, F. Sciortino, The Adam–Gibbs relation and the TIP4P/2005 model of water, Mol. Phys. 116 (21–22) (2018) 3366–3371, https://doi.org/10.1080/00268976.2018.1471230.
[44] M. Ozawa, C. Scalliet, A. Ninarello, L. Berthier, Does the Adam-Gibbs relation hold in simulated supercooled liquids? J. Chem. Phys. 151 (8) (2019) https://doi.org/10.1063/1.5113477, 084504.
[45] J.C. Dyre, T. Hechsher, K. Niss, A brief critique of the Adam–Gibbs entropy model, J. Non-Cryst. Solids 355 (10–12) (2009) 624–627, https://doi.org/10.1016/j.jnoncrysol.2009.01.039.
[46] C. Angell, S. Borick, Specific heats Cp, Cv, Cconf and energy landscapes of glassforming liquids, J. Non-Cryst. Solids 307–310 (2002) 393–406, https://doi.org/10.1016/S0022-3093(02)01500-4.
[47] A. Scala, F.W. Starr, E. La Nave, F. Sciortino, H.E. Stanley, Configurational entropy and diffusivity of supercooled water, Nature 406 (6792) (2000) 166–169, https://doi.org/10.1038/35018034.
[48] S. Saito, B. Bagchi, Thermodynamic picture of vitrification of water through complex specific heat and entropy: a journey through "no man's land", J. Chem. Phys. 150 (5) (2019) https://doi.org/10.1063/1.5079594, 054502.